Preclinical Therapy

Clinical Cancer Research

Suppression of Liver Tumor Growth and Metastasis by Adiponectin in Nude Mice through Inhibition of Tumor Angiogenesis and Downregulation of Rho Kinase/IFN-Inducible Protein 10/Matrix Metalloproteinase 9 Signaling

Kwan Man[1], Kevin T.P. Ng[1], Aimin Xu[2], Qiao Cheng[1], Chung Mau Lo[1], Jiang Wei Xiao[1], Bai Shun Sun[1], Zophia X.H. Lim[1], Jerry S. Cheung[3], Ed X. Wu[3], Chris K.W. Sun[1], Ronnie T.P. Poon[1], and Sheung Tat Fan[1]

Abstract

Purpose: We aimed to investigate the effects of adiponectin on liver cancer growth and metastasis and explore the underlying mechanisms.

Experimental Design: An orthotopic liver tumor nude mice model with distant metastatic potential was applied. Either Ad-adiponectin (1×10^8; treatment group) or Ad-luciferase (control group) was injected via portal vein after tumor implantation. Tumor growth and metastasis were monitored by Xenogen *In vivo* Imaging System. Hepatic stellate cell activation by α-smooth muscle actin staining, microvessel density by CD34 staining, macrophage infiltration in tumor tissue, and cell signaling leading to invasion, migration [Rho kinase (ROCK), IFN-inducible protein 10 (IP10), and matrix metalloproteinase 9], and angiogenesis [vascular endothelial growth factor (VEGF) and angiopoietin 1] were also compared. Tumor-nontumor margin was examined under electron microscopy. Direct effects of adiponectin on liver cancer cells and endothelial cells were further investigated by a series of functional studies.

Results: Tumor growth was significantly inhibited by adiponectin treatment, accompanied by a lower incidence of lung metastasis. Hepatic stellate cell activation and macrophage infiltration in the liver tumors were suppressed by adiponectin treatment, along with decreased microvessel density. The treatment group had less Ki-67–positive tumor cells and downregulated protein expression of ROCK1, proline-rich tyrosine kinase 2, and VEGF. Tumor vascular endothelial cell damage was found in the treatment group under electron microscopy. *In vitro* functional study showed that adiponectin not only downregulated the ROCK/IP10/VEGF signaling pathway but also inhibited the formation of lamellipodia, which contribute to cell migration.

Conclusion: Adiponectin treatment significantly inhibited liver tumor growth and metastasis by suppression of tumor angiogenesis and downregulation of the ROCK/IP10/matrix metalloproteinase 9 pathway. *Clin Cancer Res; 16(3); OF1–11. ©2010 AACR.*

Although surgical procedures such as liver resection and liver transplantation are first-line treatments for liver cancer, tumor recurrence and metastasis remain to be major problems affecting long-term disease-free survival. Therefore, development of novel adjuvant therapies targeting liver cancer growth, recurrence, and metastasis without obvious toxicity to the liver itself is essential.

Authors' Affiliations: [1]Department of Surgery and Centre for Cancer Research, [2]Department of Medicine, LKS Faculty of Medicine, and [3]Department of Electrical and Electronic Engineering, Faculty of Engineering, The University of Hong Kong, Hong Kong, P.R. China

Note: K. Man and K.T.P. Ng contributed equally to this work.

Corresponding Author: Kwan Man, Department of Surgery, The University of Hong Kong, L9-55, Faculty of Medicine Building, 21 Sassoon Road, Hong Kong, P.R. China. Phone: 852-28199646; Fax: 852-28199634; E-mail: kwanman@hkucc.hku.hk.

doi: 10.1158/1078-0432.CCR-09-1487

Adiponectin, a fat-derived hormone, has been shown to have a correlation with tumor development and prognosis (1, 2). Lower circulating levels of adiponectin have been found to be an independent predictor of colorectal cancer recurrence (3). Adiponectin can suppress hepatic stellate cell activation that plays an important role in angiogenesis. Hypoadiponectinemia accelerated liver tumor formation in a nonalcoholic steatohepatitis mouse model (4). It has been found that recombinant adiponectin not only significantly attenuated liver steatosis but also improved liver function by amelioration of inflammation (5) and rescued the marginal liver graft from acute-phase injury (6). More recent studies have also shown that adiponectin not only suppressed angiogenesis by inducing endothelial cell apoptosis (7) but also inhibited cell proliferation (8) and tumorigenesis (9). All these suggest that adiponectin, besides being a promising candidate for treating obesity-associated

Translational Relevance

In previous animal studies, we have already shown that adiponectin could attenuate small-for-size fatty liver graft injury after liver transplantation thorough anti-inflammatory response and decrease of fatty changes in the graft. In the present study, the anticancer effect of adiponectin, including suppression of tumor angiogenesis and downregulation of invasive signaling pathway, has been further confirmed in an orthotopic liver cancer model with distant metastasis potential. Therefore, adiponectin may have great potential to suppress liver tumor recurrence after surgical treatments including liver transplantation for liver cancer patients in clinical practice.

metabolic diseases, may be a potential candidate for novel therapies for liver tumor growth, recurrence, and metastasis.

Recently, there is much effort to probe the cell signaling leading to tumor invasion, angiogenesis, and metastasis. Rho kinase (ROCK) has shown its significant role in regulating cytoskeletal events and contributed to the invasion of hepatocellular carcinoma (10, 11). IFN-inducible protein 10 (IP10), which has been shown to promote tumor cell invasiveness in colon cancer (12) and related to angiogenesis in uterine cervical cancers (13), may also play potential role in hepatocellular carcinoma invasiveness. Moreover, macrophages in tumor microenvironment also play an important role in facilitating tumor invasion and angiogenesis (14) by secreting several inflammatory cytokines and chemokines, such as vascular endothelial growth factor (VEGF) and matrix metalloproteinase 9 (MMP9), which promote angiogenesis directly (15). Furthermore, in the presence of VEGF, angiopoietins may promote tumor angiogenesis and progression in human hepatocellular carcinoma (16).Therefore, it will be worthwhile to investigate the effect of adiponectin on above molecular signaling of hepatocellular carcinoma progression and invasion.

In this study, we investigated the potential anticancer effect of adiponectin on hepatocellular carcinoma through *in vitro* functional studies and with novel orthotopic liver tumor animal models with different local and distant metastatic potentials. The combined application of a novel *In vivo* Imaging System (IVIS; Xenogen IVIS 100) and the higher-resolution 7T micro–magnetic resonance imaging not only allowed longitudinal monitoring of liver tumor growth and metastasis but also provided accurate comparison of the tumor size. We also explored the underlying molecular mechanisms of adiponectin in the suppression of proliferation, invasion, migration, and angiogenesis of liver cancer cells. The significance of this study will hopefully open a new window to the development of novel therapies targeting at liver cancer growth and metastasis.

Materials and Methods

Patients. From December 2000 to November 2002, 100 patients (ages >18 years) diagnosed with hepatocellular carcinoma, which were considered to be resectable based on intraoperative ultrasonography without preoperative adjuvant therapy, were included in the current study. Other 30 cases without liver cancer were selected with control. The new tumor-node-metastasis staging and Edmonson staging of these patients was based on the clinical and pathologic diagnosis (17). The study protocol was approved by the Institutional Review Board of The University of Hong Kong. Informed consent was obtained from each patient before operation.

Cell lines. Human hepatocellular carcinoma cell lines MHCC97L (a kind gift from Liver Cancer Institute, Fudan University; ref. 18), Huh7 (a gift from Dr. H. Nakabayashi, Hokkaido University School of Medicine; ref. 19), Hep3B (American Type Culture Collection), and PLC (Japanese Cancer Research Bank) were maintained in DMEM with high glucose (Life Technologies) supplemented with 10% heat-inactivated fetal bovine serum (Life Technologies), 100 mg/mL penicillin G, and 50 μg/mL streptomycin (Life Technologies) at 37°C in a humidified atmosphere containing 5% CO_2. MHCC97L cells were stable-labeled with the luciferase gene in chromosomes. Briefly, cells were transfected with pGL3 vector (Promega), and positive clones were selected according to luciferase activity in Xenogen IVIS 100 (Xenogen; ref. 20).

Orthotopic nude mice liver tumor model. Male athymic nude mice (BALB/c *nu/nu*, 4-6 weeks old) were used. MHCC97L cells ($\sim 6 \times 10^5$) in 0.2 mL culture medium were injected subcutaneously into the right flank of each nude mouse. Once the subcutaneous tumors reached 0.8 to 1 cm in diameter, they were removed and cut into cubes $\sim$1 to 2 mm^3 in size, which were then implanted into the left liver lobes of another group of nude mice using the method described previously (21).

Treatment regimen, imaging analysis, and sample collection. Recombinant adenovirus (1×10^8 plaque-forming units) expressing adiponectin (Ad-adiponectin, treatment group) or luciferase (Ad-luciferase, control group; ref. 9) was injected via the portal vein after tumor implantation. Both the treatment group and the control group comprised 8 mice each. Blood samples were collected every week from tail vein for the detection of serum levels of adiponectin. Mice bearing liver tumors were checked by a higher-resolution 7T magnetic resonance imaging scanner, PharmaScan 70/16 (Bruker BioSpin). Liver tumor growth and lung metastasis were monitored by Xenogen IVIS every week. The nude mice were sacrificed at weeks 5, 6, and 7, respectively, after tumor implantation. Liver, lung, kidney, and spleen suspected of tumor metastasis were sampled for tissue sectioning to examine intrahepatic, lung, kidney, and spleen metastases.

Plasma level of adiponectin. Plasma levels of adiponectin of the nude mice and hepatocellular carcinoma patients together with non–hepatocellular carcinoma controls were

determined using in-house RIA as described previously (22).

Morphologic study by light and transmission electron microscopy. Liver tumor tissue including nontumor margin was taken at different time points after tumor implantation for light microscopy with H&E staining. To compare the ultrastructural features of the specimens from mice from the treatment and control groups, the specimens were immediately cut into 1-mm cubes and fixed in 2.5% glutaraldehyde in sodium carcodylate hydrochloride buffer overnight at 4°C for electron microscopy section. The sections were then examined under a transmission electron microscope, Philips EM 208 (Koninklijke Philips Electronics, 23).

Gene expression of ROCK1, IP10, angiopoietin 1, MMP9, and adiponectin receptors. Liver tumor tissue was stored at -80°C until total RNA extraction. Total RNA was extracted using RNeasy Midi kit (Qiagen). Total RNA (~0.5 μg) from each sample was used to perform reverse transcription reaction using TaqMan Reverse Transcription Reagents (ref. 24; Applied Biosystems). Reverse transcription product (1 μL) was used to perform real-time quantitative reverse transcription-PCR using TaqMan Core Reagent kit (Applied Biosystems) by ABI PRISM 7700 Sequence Detection System (Applied Biosystems). Probes and primers of ROCK, IP10, angiopoietin 1, and VEGF were purchased from Applied Biosystems. TaqMan rRNA Control Reagent (18S RNA probe and primer pair; Applied Biosystems) was used for internal control in the same PCR plate well to normalize target gene amplification copies. All samples were detected in triplicate. Readings from each sample and its internal control were used to calculate gene expression level. After normalization with the internal control, gene expression levels at different time points after liver transplantation were expressed as the folds relative to the normal liver.

The total RNA from human liver cancer cell lines (Huh7, PLC, Hep3B, MHCC97L, and MHCC97H) was also extracted using RNeasy Midi kit. The method for cDNA production was the same as for liver tumor tissues (24). Reverse transcription product (1 μL) was used to perform PCR. The primer sets for adiponectin receptor 1 are AdipoR1-F: CTTCTACTGCTCCCCACAGC and AdipoR1-R: GGTGCTTAGGAGTGGCAAAC. The primer sets for adiponectin receptor 2 are AdipoR2-F: TGTTTCGCCCAAATATCTCC and AdipoR2-R: CTGTGTGGAAGAGCCATGAA.

Protein expression of ROCK, IP10, VEGF, Akt, Bcl-2, BAX, and p53. Western blot was done with a modified version of a method described previously (25). Immunoreactive signals were visualized with ECL Plus Western Blotting Detection Reagents (Amersham Biosciences) and quantified by scanning densitometry (Syngene). Anti–ROCK-1, anti-0IP10, and anti-VEGF antibodies were purchased from Santa Cruz Biotechnology. Anti-Akt, anti–phospho-Akt (Ser^{473}), anti–Bcl-2, anti-BAX, and anti–phospho-p53 (Ser^{15}) antibodies were from Cell Signaling Technology.

Plasma levels of VEGF by ELISA. Circulating VEGF levels were detected by ELISA on plasma samples using Quantikine Mouse VEGF Immunoassay kit (R&D Systems) in accordance with a previously described method (26).

Protein expression of VEGF/proline-rich tyrosine kinase 2 and activation of macrophages and hepatic stellate cells. Paraffin sections (4 μm thick) were dewaxed in xylene, rinsed in grade alcohol, and rehydrated in water and then were placed in citric buffer (pH 6.0) and treated in a microwave oven with high power for 3 min and subsequent low power for 10 min. Afterwards, the sections underwent blocking with 3% peroxidase for 20 min and 10% goat serum for 30 min. Subsequently, primary antibodies with proper dilution were applied on the sections, which were then incubated at 4°C overnight. Following that, secondary antibodies from Dako EnVision System (DakoCytomation) were applied, and the sections were incubated for 30 min at room temperature. Signals were developed with 3,3′-diaminobenzidine substrate solution (DakoCytomation). The sections were finally counterstained by hematoxylin solution. Primary antibodies used in this study included VEGF (Santa Cruz Biotechnology), α-smooth muscle actin (DakoCytomation), CD34 (Santa Cruz Biotechnology), proline-rich tyrosine kinase 2 (Pyk2), and CD68 (BD Biosciences).

Determination of microvessel density. Microvessel density (MVD) of liver tumor tissue sections was evaluated (27). Any $CD34^+$ stained endothelial cell or endothelial cell cluster that was clearly separated from adjacent microvessels, tumor cells, and connective elements was counted as one microvessel. The mean microvessel count of the five most vascular areas was taken as the MVD, which was expressed as the absolute number of microvessels per 1.485 mm^2 (×200 field).

Determination of tumor cell apoptosis by terminal deoxynucleotidyl transferase–mediated dUTP nick end labeling assay. Paraffin sections of liver biopsies from the treatment and control groups were detected for apoptotic cells by *In Situ* Cell Death Detection kit (Roche Molecular Biochemicals, Roche Applied Science) according to the manufacturer's protocol.

Tube formation assay. Liquefied Matrigel (BD Biosciences) was used to coat the surface of the wells of a 96-well plate and allowed to solidify in a culture incubator at 37°C for 4 h. Each 30,000 cells of mouse endothelial cell line CRL2279 (American Type Culture Collection) were seeded into the precoated wells of the 96-well plate. Recombinant adiponectin protein generated from human embryonic kidney cells (5) was administered to the endothelial cells at the concentration of 0 or 30 μg/mL. Appearance of the cells on Matrigel was captured by digital camera after 24 and 48 h.

Ultrastructure of tumor cells under scanning electron microscopy. Tumor cells with or without adiponectin treatment grown on sterile round glass coverslips were fixed with 2.5% glutaraldehyde in 0.1 mol/L sodium cacodylate-HCl buffer (pH 7.4), quenched with 0.1 mol/L sucrose/cacodylate solution, and washed in cacolydate

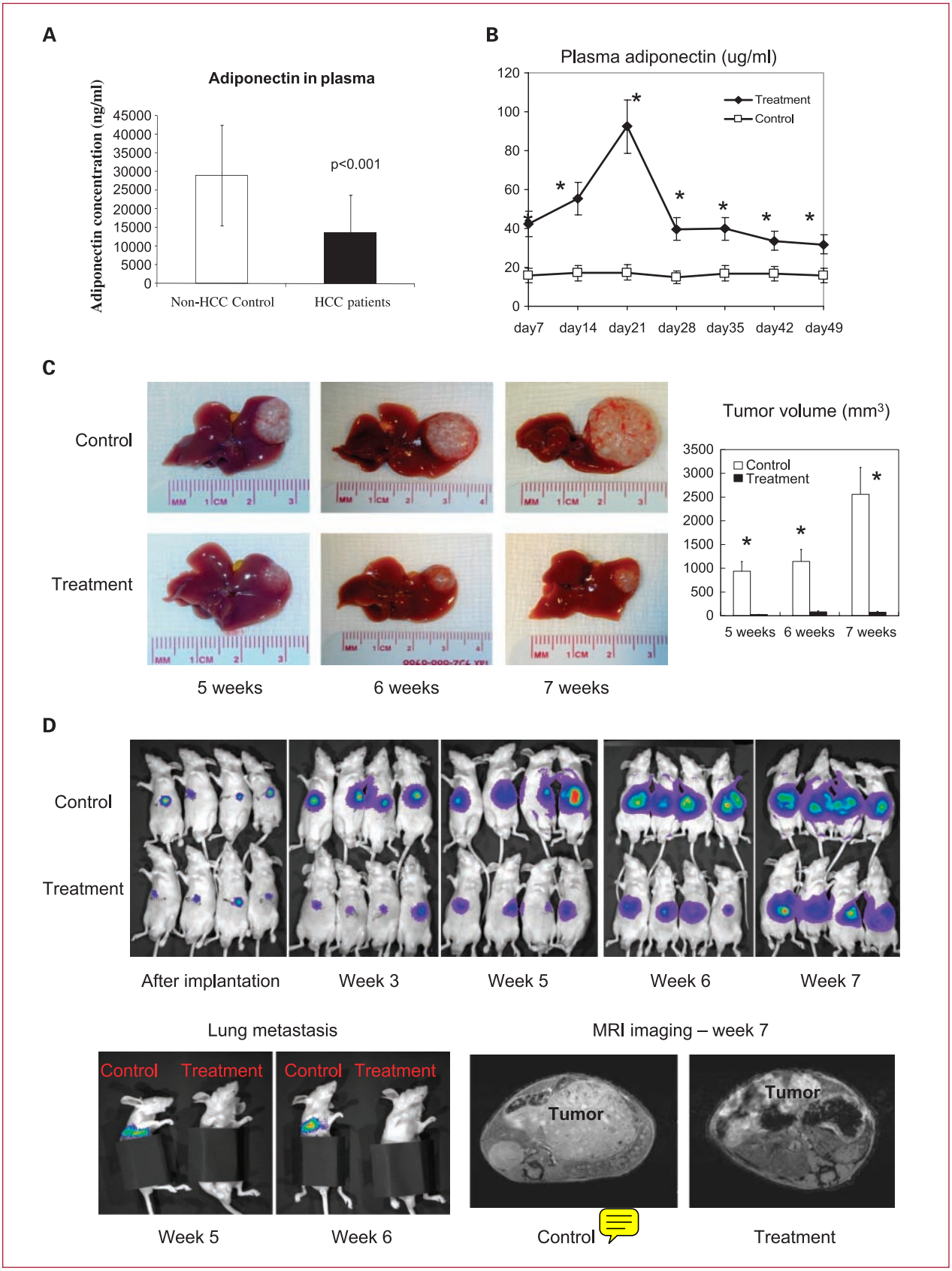
A
Adiponectin in plasma
Adiponectin concentration (ng/ml)
45000
40000
35000
30000
25000
20000
15000
10000
5000
0
p<0.001
Non-HCC Control
HCC patients
B
Plasma adiponectin (ug/ml)
120
100
80
60
40
20
0
Treatment
Control
day7
day14
day21
day28
day35
day42
day49
C
Control
Treatment
Tumor volume (mm3)
3500
3000
2500
2000
1500
1000
500
0
Control
Treatment
5 weeks
6 weeks
7 weeks
5 weeks
6 weeks
7 weeks
D
Control
Treatment
After implantation
Week 3
Week 5
Week 6
Week 7
Lung metastasis
MRI imaging – week 7
Control
Treatment
Control
Treatment
Tumor
Tumor
Week 5
Week 6
Control
Treatment

Table 1. Comparison of tumor volume and MVD-CD34 of the tumor from mice with or without adiponectin treatment

Time duration after tumor implantation	Treatment (n = 8)	Control (n = 8)	P
5 wk, tumor volume (mm^3)	25.4 (6-75)	936 (500-1,267.5)	0.002
6 wk, tumor volume (mm^3)	81.25 (6-198)	1,143 (75-2,176)	0.009
7 wk, tumor volume (mm^3)	75 (40-125)	2,560 (1,600-3,260)	0.002
5 wk, MVD-CD34/1.485 mm^2	7.52 (4.67-11.7)	38.72 (38-39.8)	0.006
6 wk, MVD-CD34/1.485 mm^2	6 (2-11.25)	28 (15-37)	0.000
7 wk, MVD-CD34/1.485 mm^2	8.25 (4-9)	35.6 (26.5-52.7)	0.004

NOTE: Median (range).

buffer. The samples were then postfixed with 1% OsO_4 in cacodylate buffer. After a cacodylate buffer wash, they were dehydrated through a graded series of ethanol washes followed by critical point drying using BAL-TEC CPD 030 Critical Point Dryer (BAL-TEC). The samples were then sputter-coated with a layer of gold using BAL-TEC SCD 005 Sputter Coater (BAL-TEC) and visualized using Leica Cambridge Stereoscan 440 SEM (Leica) at an accelerating voltage of 12 kV.

Statistical analysis. Continuous variables were expressed as median with range. Mann-Whitney *U* test was used for statistical comparison. χ^2 test was used to compare incidence of lung metastasis in the nude mice orthotopic liver tumor model and to compare incidence of venous invasion as well as incidence of tumor thrombus in the rat transplantation model. Calculations were made with SPSS computer software (SPSS).

Results

Plasma levels of adiponectin were decreased in hepatocellular carcinoma patients. Preoperative plasma levels of adiponectin of the hepatocellular carcinoma patients were significantly decreased compared with that of the non–hepatocellular carcinoma controls [11.04 (0-48.24) versus 30.85 (0-46.32) μg/mL; P = 0.000; Fig. 1A]. However, there was no statistical difference of the correlation among the adiponectin levels and clinicopathologic parameters in the hepatocellular carcinoma patients. F1

Ad-adiponectin injection significantly increased circulating adiponectin levels during the first 5 weeks after treatment. Without Ad-adiponectin treatment, circulating adiponectin levels were constantly maintained at ~15 μg/mL (Fig. 1B). Ad-adiponectin portal vein injection significantly increased circulating adiponectin levels during the whole duration after treatment. The levels increased to ~3-fold compared with those in the control group in the first 7 days and reached the peak level (6-fold) at day 21 after treatment. Consistently higher circulating levels of adiponectin played an important role in inhibition of liver tumor growth and metastasis as shown in Fig. 1C and D.

Adiponectin significantly suppressed liver tumor growth and metastasis. Liver tumor growth and metastasis were compared between animals with and without adiponectin treatment. Direct measurement of tumor volume was done at weeks 5, 6, and 7 after orthotopic tumor implantation (Fig. 1C; Table 1). Longitudinal monitoring of tumor growth and metastasis by Xenogen IVIS and 7T micro–magnetic resonance imaging (Fig. 1D) showed that adiponectin significantly inhibited liver tumor growth and lung metastasis after treatment. Local metastasis (intrahepatic) and distant metastasis (lung) were confirmed by histology examination (Fig. 1D). Magnetic resonance imaging scanning also showed the significant decrease of tumor size at week 7 after tumor implantation (Fig. 1D). After adiponectin treatment, incidence of intrahepatic metastasis decreased from 87.5% (7 of 8) to 25% (2 of 8; P = 0.041). Similarly, there was significant inhibition of lung metastasis by adiponectin treatment, manifested by a drop of incidence from 75% (6 of 8) to 12.5% (1 of 8; P = 0.041). T1

Adiponectin attenuated invasive growth pattern of tumor. Under light microscope examination (Fig. 2A), invasive tumor growth patterns manifested by the presence of tumor thrombus, intrahepatic metastasis, and lung metastatic F2

Fig. 1. A, comparison of plasma levels of adiponectin between hepatocellular carcinoma patients and non–hepatocellular carcinoma controls. Significantly lower levels of adiponectin were found in hepatocellular carcinoma patients (P < 0.001). B, comparison of plasma adiponectin levels of mice with and without adiponectin treatment at different time points after tumor implantation. Significantly higher levels of adiponectin were found during the 49 days after tumor implantation. *, P < 0.01, compared with control group. C, comparison of *in situ* tumor growth and tumor volume with and without adiponectin treatment in an orthotopic liver tumor nude mice model at weeks 5, 6, and 7 after tumor implantation. D, monitoring of *in situ* tumor growth by Xenogen IVIS at different time points after tumor implantation. Orthotopic liver tumor growth and lung metastasis was inhibited by adiponectin treatment. Representative magnetic resonance imaging at week 7 after tumor implantation showed the difference of tumor size between mice with and without adiponectin treatment. The liver tumor shows hyperdensity compared with normal tissues.

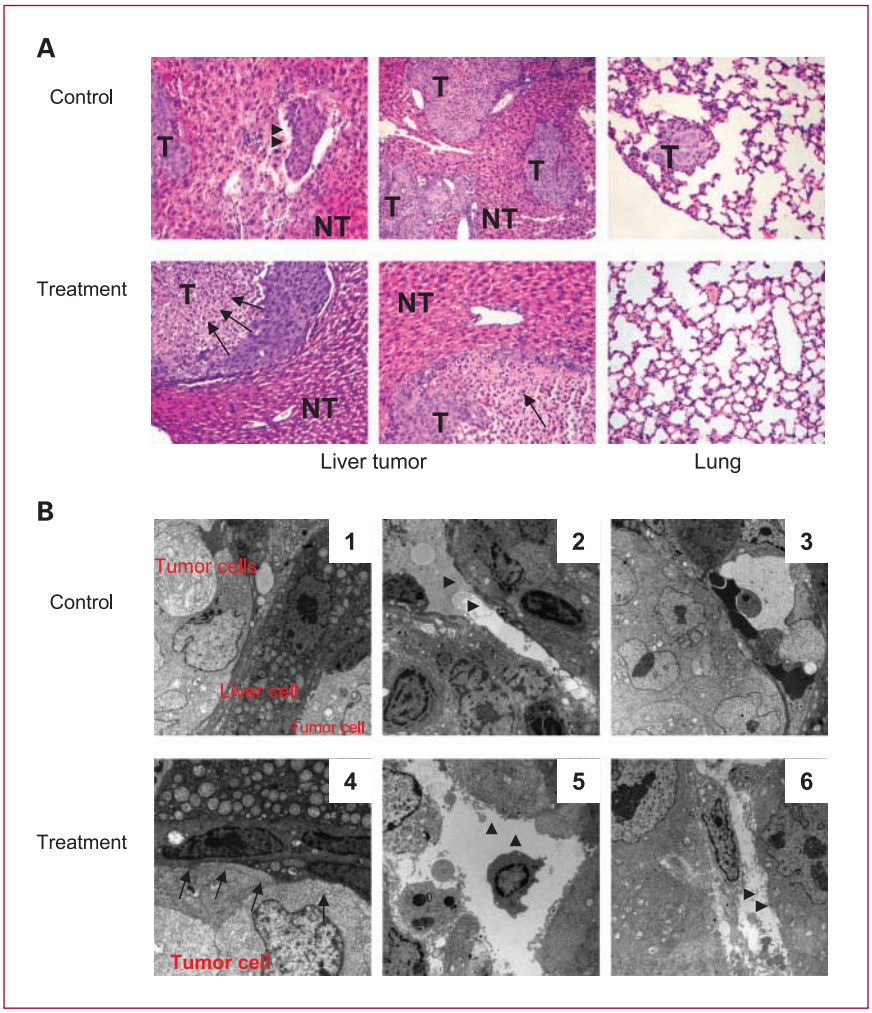

Fig. 2. A, histologic features of liver tumors from mice with and without adiponectin treatment. Invasive growth pattern together with tumor thrombus (arrowheads) was found in the control group. Lung metastatic nodule (*T*) was also present in the control group. In the treatment group, obvious tumor necrosis was present (arrows). B, ultrastructure of liver tumor by electron microscopy. Invasive tumor growth (1) and intact tumor endothelial cells (2) together with direct tumor cell invasion to blood vessel (3) were found in the control group. After adiponectin treatment, clear margin between tumor and nontumor cells (4) together disruption of tumor endothelial cells (5 and 6) was shown in the treatment group.

nodules were shown in the control group. After adiponectin treatment, clear demarcation between tumor tissue and nontumor tissue was present together with obvious tumor necrosis. Consistently, ultrastructural changes (Fig. 2B) in liver tumor tissue and nontumor tissue were obvious after adiponectin treatment. In the control group where intrahepatic metastasis was seen (Fig. 2B-1), tumor endothelial cells were intact (Fig. 2B-2) and tumor cells invaded blood vessels directly (Fig. 2B-3). In the treatment group, clear margin between tumor cells and liver cells was observed (Fig. 2B-4), and disruption of tumor endothelial cells (Fig. 2B-5 and 6) was shown in most of the cases. The disruption of tumor endothelial cells might have contributed to inhibition of tumor angiogenesis.

Adiponectin significantly attenuated hepatic stellate cell activation and decreased MVD. Hepatic stellate cell activation in liver tumors was considered to be related to tumor angiogenesis (28). Without adiponectin treatment, remarkable activation of hepatic stellate cells indicated by α-smooth muscle actin staining was found in the liver tumors at different time points after tumor implantation (Fig. 3A). Adiponectin treatment significantly inhibited F3
the hepatic stellate cell activation in the liver tumors (Fig. 3A). Consistently, tumor MVD calculated by new vessel formation using CD34 staining decreased significantly after adiponectin treatment (Fig. 3B; Table 1).

Adiponectin suppressed Pyk2 expression and induced tumor cell apoptosis. Pyk2 has recently been found to be relating to liver tumor invasion and poor prognosis in clinical study (29) and to promote proliferation and invasiveness of hepatocellular carcinoma cells through c-Src/extracellular signal-regulated kinase activation (20, 23). In the current animal study, intracellular protein expression of Pyk2 in liver tumors was downregulated by adiponectin at different time points after treatment (Fig. 3C). Furthermore, adiponectin treatment induced significant tumor cell apoptosis compared with the control group (Fig. 3D) at different time points.

Adiponectin downregulated ROCK/IP10/angiopoietin 1/MMP9/VEGF cell signaling in tumor tissue. mRNA expression levels of ROCK, IP10, angiopoietin 1, and MMP9 in liver tumor tissue were compared between mice with

F4 and without treatment (Fig. 4A). There were 6 animals included in each group for the analysis. Adiponectin significantly downregulated gene expression levels of ROCK, IP10, angiopoietin 1, and MMP9 in liver tumors at different time points after treatment. Consistently, protein expression of ROCK1 and VEGF was also found downregulated after adiponectin treatment by Western blot (Fig. 4B). In the control group, during the 5 to 7 weeks after tumor implantation, immunostaining revealed strong signals of intracellular protein expression of VEGF in the liver tumors (Fig. 4C). On the contrary, only weak VEGF expression was detected together with tumor necrosis in the treatment group. Consistently, circulating serum VEGF levels descended significantly at weeks 5, 6, and 7 in the treatment group (Fig. 4D). Consistent with the downregulation of cell signaling leading to tumor cell invasion and angiogenesis, tumor-associated macrophage infiltration was also decreased after adiponectin treatment (Fig. 4C).

Effect of adiponectin on apoptotic signaling and ROCK/IP10/VEGF pathway in liver cancer cells and inhibition of tube formation of tumor endothelial cells. Adiponectin

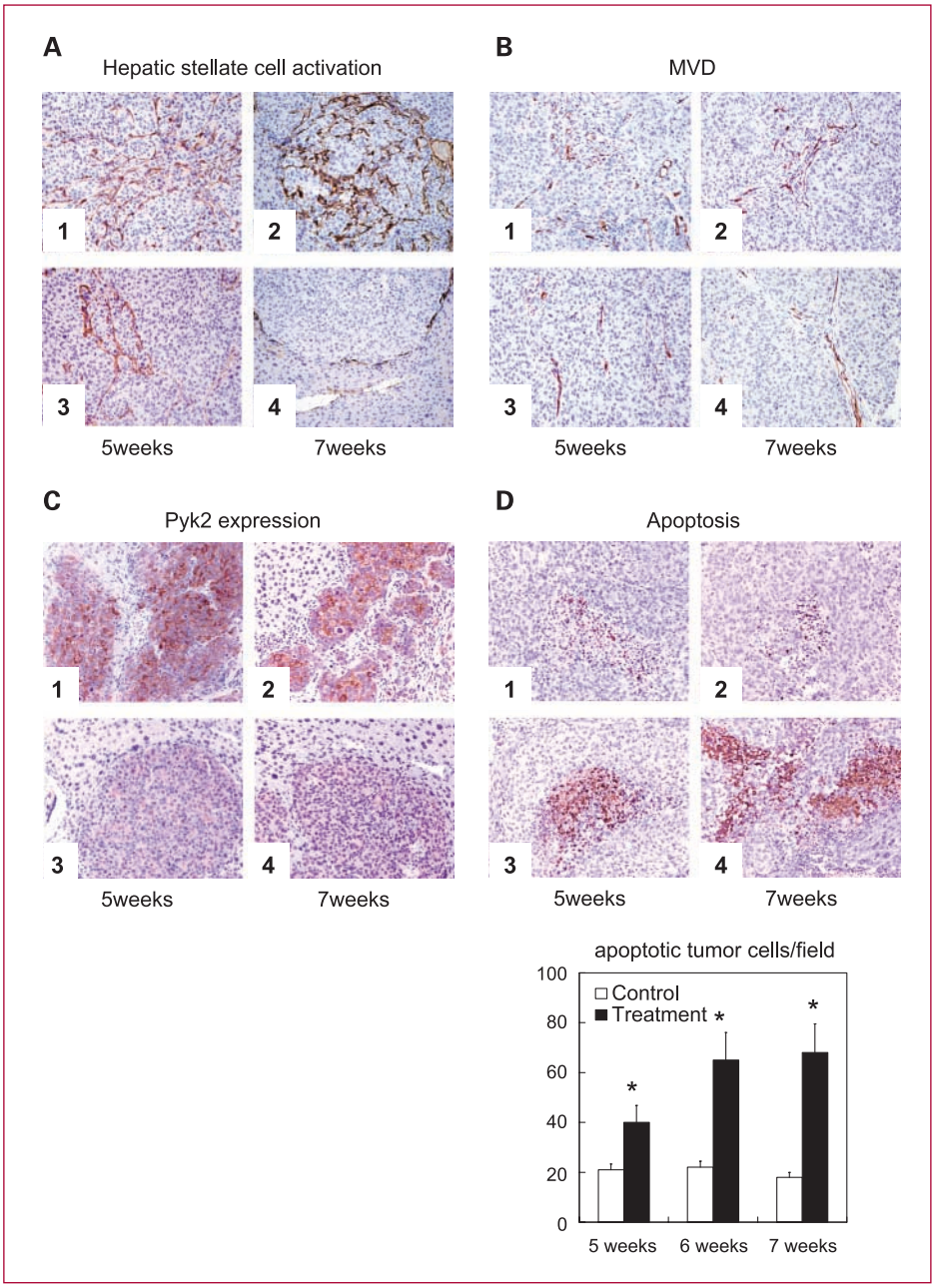

Fig. 3. A, comparison of hepatic stellate cell activation in liver tumors from mice with and without treatment was detected by immunostaining of α-smooth muscle actin. 1 and 2, control group; 3 and 4, treatment group. B, comparison of MVD by $CD34^+$ tumor endothelial cells by immunostaining between mice with and without treatment. 1 and 2, control group; 3 and 4, treatment group. C, intracellular protein expression of Pyk2 in liver tumor was examined by immunostaining. 1 and 2, control group; 3 and 4, treatment group. D, tumor cell apoptosis was compared by terminal deoxynucleotidyl transferase–mediated dUTP nick end labeling staining. Comparison of apoptotic tumor cells of mice with and without treatment at different time points. 1 and 2, control group; 3 and 4, treatment group. *, $P < 0.05$, comparison between treatment and control groups.

receptors 1 and 2 were expressed in all human liver cancer cell lines in the current study (Fig. 5A-1). The gene expression levels of these two receptors were consistent after adiponectin administration (with similar expression levels by real-time quantitative reverse transcription-PCR; data no shown). The effect of adiponectin on apoptotic signaling of PLC (invasive hepatocellular carcinoma cell line) and MHCC97L (metastatic cell line) cells were investigated by Western blot (Fig. 5A-2). The downregulation of Akt signal and upregulation of BAX/P53 were mainly found in PLC cell line. Adiponectin administration (of both adenovirus and protein) downregulated the protein expression of ROCK, IP10, and VEGF in MHCC97L liver tumor cells in a dose-dependent manner (Fig. 5B). Adiponectin protein also inhibited the tube formation ability of mouse endothelial cells (cell line CRL2279) in tube formation assay (Fig. 5C).

Adiponectin treatment decreased lamellipodial formation on tumor cell surface. Without adiponectin treatment, obvious lamellipodial formation was found on MHCC97L liver tumor cell surface (Fig. 5D). After administration of adiponectin protein at different concentrations, formation of lamellipodia was inhibited on tumor cell surface (Fig. 5D).

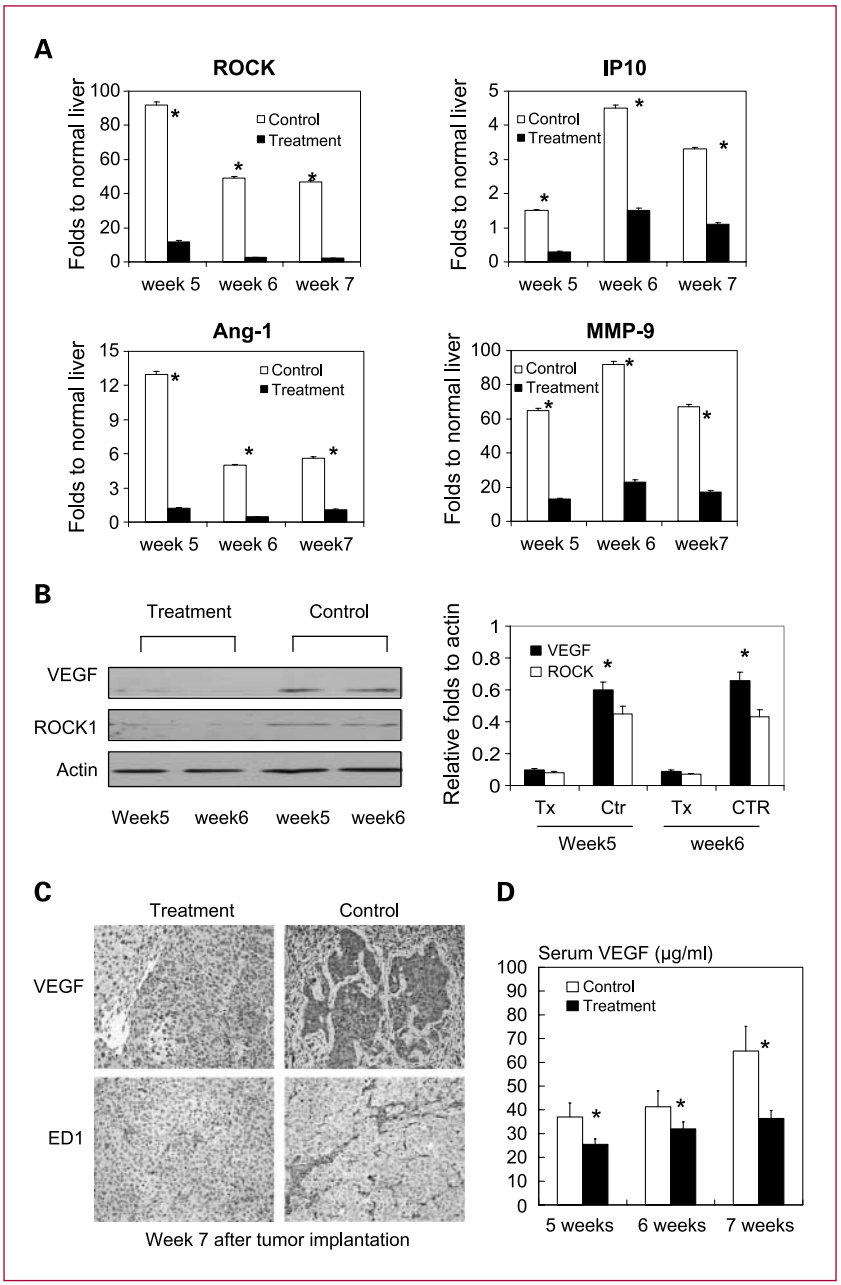

Fig. 4. A, gene expression of cell signaling leading to tumor invasion and angiogenesis in tumor tissue detected by real-time quantitative reverse transcription-PCR. B, protein expression of VEGF and ROCK1 in liver tumor detected by Western blot. C, intracellular protein expression of VEGF and macrophage infiltration (ED1 staining) in the liver tumor. D, serum levels of circulating VEGF were compared by quantitative ELISA. *, $P < 0.05$, compared with control group. There were 6 animals included in each group for analysis.

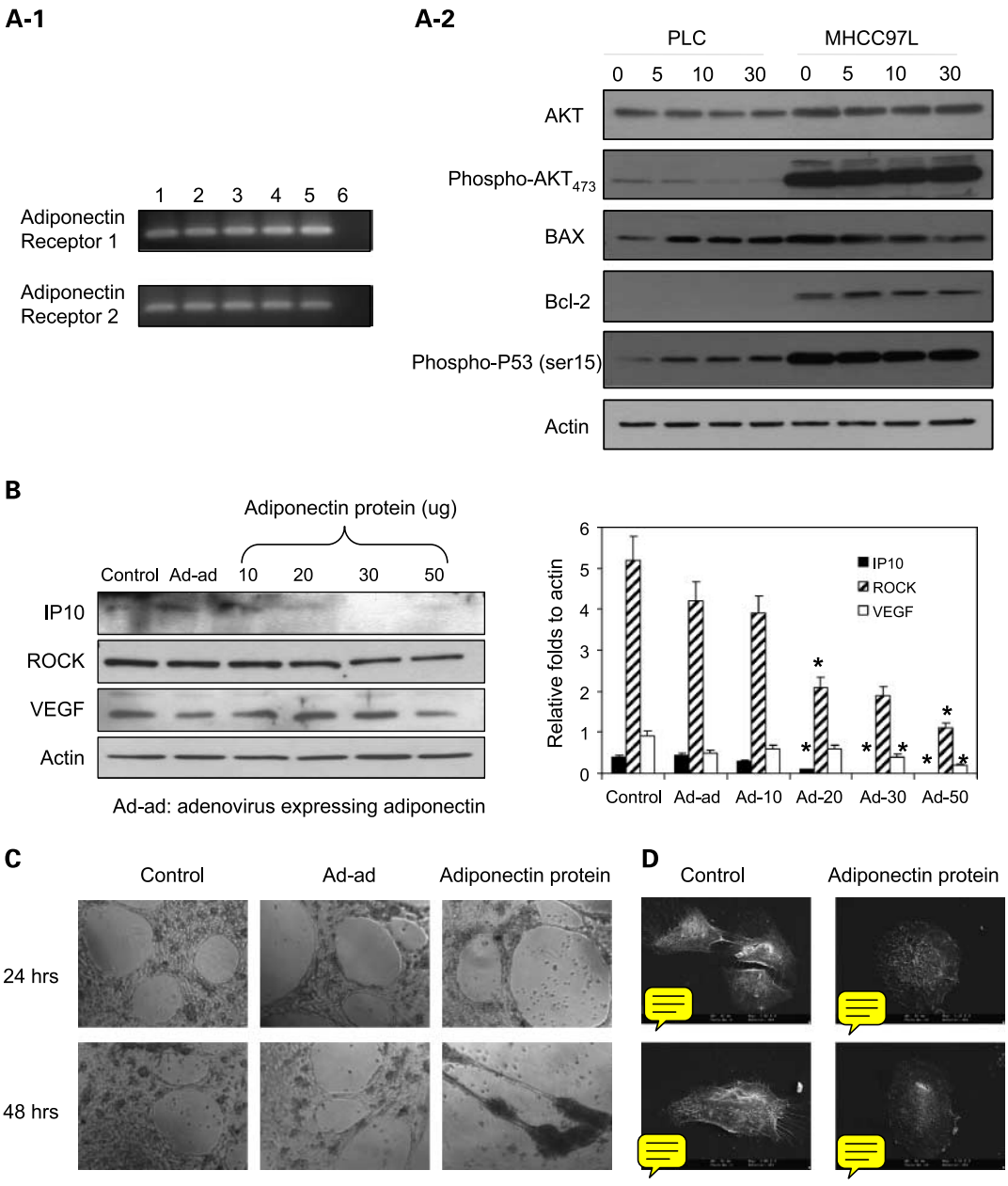

Fig. 5. A-1, gene expression of adiponectin receptors 1 and 2 in different liver cancer cell lines. 1, PLC; 2, Huh7; 3, Hep3B; 4, MHCC97L; 5, MHCC97H; 6, negative control. A-2, cell signaling leading to apoptosis was compared in PLC and MHCC97L cell lines under 5, 10, and 30 μg adiponectin protein administration for 24 h. B, protein expression of ROCK, IP10, and VEGF was compared in MHCC97L cells under adiponectin treatment. Ad-ad, adenovirus with adiponectin expression. There were 6 animals included in each group for analysis. C, comparison of tube formation in mouse endothelial cells (cell line CRL2279) with or without adiponectin administration. D, comparison of lamellipodial formation on tumor cell surface. Without adiponectin treatment, obvious lamellipodial formation was found on MHCC97L liver tumor cell surface (a and b). After administration of adiponectin protein at concentrations of 50 μg (c and d), only a few lamellipodia were formed on the tumor cell surface.

Discussion

Recent clinical case-control studies have shown the significant association between lower circulating adiponectin levels and poor prognosis (1). It has also been reported that hypoadiponectinemia promoted tumorigenesis in a mouse liver tumor model with nonalcoholic steatohepatitis (4). In our clinical series, significant lower plasma levels of adiponectin were found in the hepatocellular carcinoma patients compared with the non–hepatocellular carcinoma controls.

Therefore, it is worthwhile to study the anticancer effect of adiponectin on liver tumor growth and metastasis and to explore the underlying molecular mechanism therein.

In this study, the significant effect of adiponectin in inhibition of tumor growth and metastasis was first shown in an orthotopic liver tumor model with distant metastatic potential. With the application of Xenogen IVIS and higher-resolution micro–magnetic resonance imaging, remarkable suppression of *in situ* liver tumor growth by adiponectin treatment was shown longitudinally at different time points. In addition to the inhibition of liver tumor growth, adiponectin treatment also significantly decreased the incidence of local and distant metastasis. Consistent with the phenotype of tumor growth and metastasis, histologic finding also showed that invasive growth pattern, the manifestation of which included tumor thrombus and intrahepatic metastasis, was mainly present in the control group. After adiponectin treatment, obvious tumor necrosis and clear margin between tumor and nontumor were observed. Electron microscopy revealed that adiponectin treatment destroyed the integrity of tumor endothelial cells. This phenomenon was consistent with the presence of suppression of tumor angiogenesis. Without treatment, tumor ultrastructure showed capillarized sinusoids and tumor cells were invading vessels, two typical features linked to tumor angiogenesis and invasiveness (30, 31).

In the study, suppression of tumor growth, invasiveness, and angiogenesis might have been directly caused by the downregulation of liver tumor gene expression profiles by adiponectin. Such profiles prompt cell invasion and migration signaling IP10/ROCK/Pyk2 (12, 28, 29, 32–34). When comparing the treatment and control groups, it was found that, in addition to the effects of adiponectin on cell signaling leading to invasion and migration, adiponectin also inhibited tumor-associated macrophage infiltration in liver tumors. Macrophages in tumor microenvironment play an important role in facilitating tumor invasion and angiogenesis (14) by secreting several inflammatory cytokines and chemokines, such as VEGF and MMP9, which promote angiogenesis directly (15). The phenomenon of inhibition of tumor-associated macrophages by adiponectin was consistent with the downregulation of VEGF and MMP9 expressions in tumor tissue. It was also consistent with the decrease of MVD and the attenuation of tumor-associated hepatic stellate cell activation, which are also considered to play direct roles in tumor angiogenesis and metastasis (28, 35). Furthermore, significantly lower circulating VEGF levels were also shown in the current *in vivo* animal model. Obviously, liver tumor growth and metastasis were significantly suppressed by adiponectin treatment.

The direct effect of adiponectin in inhibition of liver tumor invasion and angiogenesis was further confirmed in our current *in vitro* functional studies. The *in vitro* functional studies clearly indicated that adiponectin directly diminished lamellipodial formation on cell surface, which is the typical characteristic leading to cell motility (36). In addition to the alteration of tumor cell surface structure, adiponectin also downregulated intracellular protein levels of IP10/ROCK/VEGF in a dose-dependent manner. This finding was consistent with the phenotype of our animal models with suppressed tumor growth and metastasis. Furthermore, adiponectin not only targeted liver tumor cells directly but also inhibited tube formation of endothelial cells, which is involved in tumor angiogenesis. It was further confirmed that adiponectin suppressed tumor angiogenesis in the current orthotopic liver cancer mouse model. Although the significant apoptosis of tumor cells was found after adiponectin treatment in the animal model, the *in vitro* functional study in MHCC97L did not confirm the downregulation of Akt signaling by adiponectin. Therefore, the induction of apoptosis by adiponectin might be the secondary effect from antiangiogenesis rather than its direct effect in MHCC97L cells. However, the downregulation of Akt signal and upregulation of BAX/P53 were found in PLC cell line. It suggested that the effect of adiponectin-inducing apoptosis might be cell line dependent.

In conclusion, adiponectin has shown its great potential in suppression of liver tumor growth and metastasis through downregulation of cell signaling leading to invasion and angiogenesis. In addition, it inhibits tumor inflammatory response by suppressing tumor-associated macrophage infiltration. These suggest that adiponectin may be a promising candidate for potential adjuvant therapies for treating liver cancer before or after liver surgery in prevention of late-phase tumor recurrence.

Disclosure of Potential Conflicts of Interest

No potential conflicts of interest were disclosed. Q3

Grant Support

Seed Funding Programme for Basic Research, University of Hong Kong.

The costs of publication of this article were defrayed in part by the payment of page charges. This article must therefore be hereby marked *advertisement* in accordance with 18 U.S.C. Section 1734 solely to indicate this fact.

Received 6/10/09; revised 11/26/09; accepted 12/2/09.

References

1. Michalakis K, Williams CJ, Mitsiades N, et al. Serum adiponectin concentrations and tissue expression of adiponectin receptors are reduced in patients with prostate cancer: a case control study. Cancer Epidemiol Biomarkers Prev 2007;16:308–13.
2. Spyridopoulos TN, Petridou ET, Skalkidou A, Dessypris N, Chrousos GP, Mantzoros CS. Low adiponectin levels are associated with renal cell carcinoma: a case-control study. Int J Cancer 2007;120:1573–8.
3. Ferroni P, Palmirotta R, Spila A, et al. Prognostic significance of

adiponectin levels in non-metastatic colorectal cancer. Anticancer Res 2007;27:483–9.
4. Kamada Y, Matsumoto H, Tamura S, et al. Hypoadiponectinemia accelerates hepatic tumor formation in a nonalcoholic steatohepatitis mouse model. J Hepatol 2007
5. Xu A, Wang Y, Keshaw H, Xu LY, Lam KS, Cooper GJ. The fat-derived hormone adiponectin alleviates alcoholic and nonalcoholic fatty liver diseases in mice. J Clin Invest 2003;112:91–100.
6. Man K, Zhao Y, Xu A, et al. Fat-derived hormone adiponectin combined with FTY720 significantly improves small-for-size fatty liver graft survival. Am J Transplant 2006;6:467–76.
7. Brakenhielm E, Veitonmaki N, Cao R, et al. Adiponectin-induced antiangiogenesis and antitumor activity involve caspase-mediated endothelial cell apoptosis. Proc Natl Acad Sci U S A 2004;101:2476–81.
8. Wang Y, Lam KS, Xu JY, et al. Adiponectin inhibits cell proliferation by interacting with several growth factors in an oligomerization-dependent manner. J Biol Chem 2005;280:18341–7.
9. Wang Y, Lam JB, Lam KS, et al. Adiponectin modulates the glycogen synthase kinase-3β/β-catenin signaling pathway and attenuates mammary tumorigenesis of MDA-MB-231 cells in nude mice. Cancer Res 2006;66:11462–70.
10. Wong CC, Wong CM, Tung EK, Man K, Ng IO. Rho-kinase 2 is frequently overexpressed in hepatocellular carcinoma and involved in tumor invasion. Hepatology 2009;49:1583–94.
11. Wong CC, Wong CM, Ko FC, et al. Deleted in liver cancer 1 (DLC1) negatively regulates Rho/ROCK/MLC pathway in hepatocellular carcinoma. PLoS ONE 2008;3:e2779.
12. Zipin-Roitman A, Meshel T, Sagi-Assif O, et al. CXCL10 promotes invasion-related properties in human colorectal carcinoma cells. Cancer Res 2007;67:3396–405.
13. Sato E, Fujimoto J, Toyoki H, et al. Expression of IP-10 related to angiogenesis in uterine cervical cancers. Br J Cancer 2007;96:1735–9.
14. Condeelis J, Pollard JW. Macrophages: obligate partners for tumor cell migration, invasion, and metastasis. Cell 2006;124:263–6.
15. Coussens LM, Tinkle CL, Hanahan D, Werb Z. MMP-9 supplied by bone marrow-derived cells contributes to skin carcinogenesis. Cell 2000;103:481–90.
16. Mitsuhashi N, Shimizu H, Ohtsuka M, et al. Angiopoietins and Tie-2 expression in angiogenesis and proliferation of human hepatocellular carcinoma. Hepatology 2003;37:1105–13.
17. Ng KT, Man K, Sun CK, et al. Clinicopathological significance of homeoprotein Six1 in hepatocellular carcinoma. Br J Cancer 2006;95:1050–5.
18. Li Y, Tang ZY, Ye SL, et al. Establishment of cell clones with different metastatic potential from the metastatic hepatocellular carcinoma cell line MHCC97. World J Gastroenterol 2001;7:630–6.
19. Nakabayashi H, Taketa K, Miyano K, Yamane T, Sato J. Growth of human hepatoma cells lines with differentiated functions in chemically defined medium. Cancer Res 1982;42:3858–63.
20. Sun CK, Man K, Ng KT, et al. Proline-rich tyrosine kinase 2 (Pyk2) promotes proliferation and invasiveness of hepatocellular carcinoma cells through c-Src/ERK activation. Carcinogenesis 2008;29:2096–105.
21. Lee TK, Man K, Ho JW, et al. FTY720: a promising agent for treatment of metastatic hepatocellular carcinoma. Clin Cancer Res 2005;11:8458–66.
22. Xu A, Yin S, Wong L, Chan KW, Lam KS. Adiponectin ameliorates dyslipidemia induced by the human immunodeficiency virus protease inhibitor ritonavir in mice. Endocrinology 2004;145:487–94.
23. Man K, Lo CM, Xiao JW, et al. The significance of acute phase small-for-size graft injury on tumor growth and invasiveness after liver transplantation. Ann Surg 2008;247:1049–57.
24. Man K, Fan ST, Lo CM, et al. Graft injury in relation to graft size in right lobe live donor liver transplantation: a study of hepatic sinusoidal injury in correlation with portal hemodynamics and intragraft gene expression. Ann Surg 2003;237:256–64.
25. Man K, Su M, Ng KT, et al. Rapamycin attenuates liver graft injury in cirrhotic recipient—the significance of down-regulation of Rho-ROCK-VEGF pathway. Am J Transplant 2006;6:697–704.
26. Man K, Lo CM, Ng IO, et al. Liver transplantation in rats using small-for-size grafts: a study of hemodynamic and morphological changes. Arch Surg 2001;136:280–5.
27. Poon RT, Ng IO, Lau C, et al. Tumor microvessel density as a predictor of recurrence after resection of hepatocellular carcinoma: a prospective study. J Clin Oncol 2002;20:1775–85.
28. Man K, Ng KT, Lo CM, et al. Ischemia-reperfusion of small liver remnant promotes liver tumor growth and metastases—activation of cell invasion and migration pathways. Liver Transpl 2007;13:1669–77.
29. Sun CK, Ng KT, Sun BS, et al. The significance of proline-rich tyrosine kinase2 (Pyk2) on hepatocellular carcinoma progression and recurrence. Br J Cancer 2007;97:50–7.
30. Ho JW, Man K, Sun CK, Lee TK, Poon RT, Fan ST. Effects of a novel immunomodulating agent, FTY720, on tumor growth and angiogenesis in hepatocellular carcinoma. Mol Cancer Ther 2005;4:1430–8.
31. Nagy JA, Brown LF, Senger DR, et al. Pathogenesis of tumor stroma generation: a critical role for leaky blood vessels and fibrin deposition. Biochim Biophys Acta 1989;948:305–26.
32. Croft DR, Sahai E, Mavria G, et al. Conditional ROCK activation *in vivo* induces tumor cell dissemination and angiogenesis. Cancer Res 2004;64:8994–9001.
33. Itoh S, Maeda T, Shimada M, et al. Role of expression of focal adhesion kinase in progression of hepatocellular carcinoma. Clin Cancer Res 2004;10:2812–7.
34. Lipinski CA, Tran NL, Menashi E, et al. The tyrosine kinase Pyk2 promotes migration and invasion of glioma cells. Neoplasia 2005;7:435–45.
35. Olaso E, Salado C, Egilegor E, et al. Proangiogenic role of tumor-activated hepatic stellate cells in experimental melanoma metastasis. Hepatology 2003;37:674–85.
36. Bowden ET, Onikoyi E, Slack R, et al. Co-localization of cortactin and phosphotyrosine identifies active invadopodia in human breast cancer cells. Exp Cell Res 2006;312:1240–53.